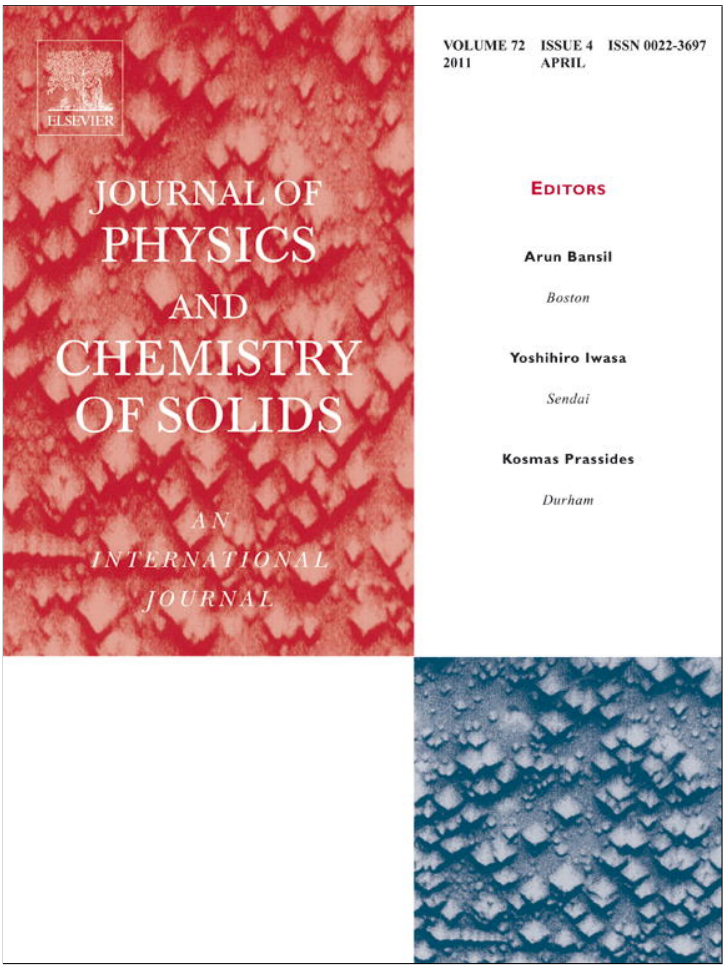

Journal of Physics and Chemistry of Solids 72 (2011) 236–244

Contents lists available at ScienceDirect

Journal of Physics and Chemistry of Solids

journal homepage: www.elsevier.com/locate/jpcs

Phase transitions in $CsHSO_4$ up to 2.5 GPa: Impedance spectroscopy under pressure

Nikolai Bagdassarov *

Institute for Geosciences, Goethe-University in Frankfurt am Main, Altenhöferallee 1, D-60438 Frankfurt am Main, Germany

ARTICLE INFO

Article history:
Received 17 May 2010
Received in revised form
30 November 2010
Accepted 13 January 2011
Available online 26 January 2011

Keywords:
C. high pressure
D. electrical conductivity
D. phase equilibria

ABSTRACT

Phase transitions in $CsHSO_4$ at pressures up to 2.5 GPa have been studied with the help of electrical impedance measurements. The phase boundaries have been identified with the help of calculated activation energies of electrical conductivity and dielectric relaxation time. The derived temperatures of phase transition from the low conductive phase II into super ionic phase I at pressure less than 1 GPa confirm the previous results of Ponyatovskiĭ et al. (1985) [4] and Friesel et al. (1989) [27]. The phase diagram derived in this study for pressure larger than 1 GPa differs from the data of Ponyatovskiĭ et al. (1985) [4]. The phase transitions IV–VI and VI–I occur at higher temperatures having significantly larger Clapeyron slope. The phase VII was not identified from heating cycle and appears only under cooling between phases I and VI. The phase VIII was detected at 2.5 GPa at $T<350$ K and only during heating.

1. Introduction

During the last two decades there is a growing interest for fast protonic conductors because of their potential applications in fuel cells, gas sensors, hydrogen/water reactors, etc. [1,2]. $CsHSO_4$ crystals represents a special interest among other fast protonic conductors due to their highest conductivity in the high temperature phase [3–6], which possesses protonic electrical conductivity because of the enhanced translational mobility of protons above the phase transition temperature, $T>T_c$. The phase transition temperature T_c corresponds to the phase boundary between the monoclinic, low temperature phase II ($P2_1/c$), and the tetragonal, high temperature phase I ($I4_1/amd$). T_c has been determined at the atmospheric pressure 413–414 K according to [3,6,7], 415 K [8], 416 K [9–11] and 417 K [5]. Different methods used to identify this phase transition temperature resulted in small variations of T_c: 413 K according to electrical conductivity measurements and 417–419 K according to DSC data [12,13]. There are only few experimental works dealing with determination of T_c at pressure. In [10,14] the DTA method has been realized at pressures up to 0.9 GPa. Today, the consensus exists on the low pressure part of the phase diagram $CsHSO_4$ at $P<0.9$ GPa [4,10,14]. The measurements indicate a small positive slope of Clapeyron slope of this phase boundary from 5 K/GPa [4] to 12.6 K/GPa [14]. The phase diagram at higher pressures (up to 2 GPa) has been explored only once in [4] using a constant frequency AC-electrical conductivity measurements and piezometry. To the author knowledge this is only one publication of the phase diagram $CsHSO_4$ at high pressures which was estimated about 25 years ago. The phase diagram of $CsHSO_4$ has been widely exploited in many theoretical studies and some new high pressure polymorphs of $CsHSO_4$ have been predicted, but the high pressure–high temperature results of Ponyatovskiĭ et al. [4] have not been reproduced or verified experimentally. As a matter of fact in [4] the measured Clapeyron slope of the phase transition I–II below 1 GPa corresponds to the entropy change $\Delta S=82$ J/mol/K, which is five times larger than the latter experimentally measured and theoretically calculated $\Delta S=12$–15 J/mol/K for this phase boundary [15]. The data of [4,14] indicate a small thermal hysteresis (ca. 4 K) of the phase transition in superprotonic phase I at $P<1$ GPa. The results of Ponyatovskiĭ et al. [4] at higher pressures indicate no thermal hysteresis although that the phase transition II–I is the pronounced first order of the phase transition and the thermal hysteresis should not be negligible.

In the present study the impedance spectroscopy (IS) method has been implemented to measure the bulk ionic electrical conductivity of $CsHSO_4$ at pressures up to 2.5 GPa. The implied impedance spectroscopy and the results which are obtained in this study provide not only specific resistance of the studied sample, but also the dielectric relaxation time of $CsHSO_4$ different polymorphs which has not been reported before.

2. Experiments

2.1. Sample preparation

The crystals of $CsHSO_4$ have been synthesized by slow evaporation of a mixture with molar ratio 1:1 of Cs_2SO_4 and H_2SO_4

* Tel.: +49 69 798 40126; fax: +49 69 79840131.
E-mail address: nickbagd@geophysik.uni-frankfurt.de

0022-3697/$ - see front matter © 2011 Elsevier Ltd. All rights reserved.
doi:10.1016/j.jpcs.2011.01.008

1 M-water solutions over 14 days. The crystals of $CsHSO_4$ have been dried and grounded to a fine powder with ca. 20–30 μm of grain size. The purity of the starting and the recovered after high pressure experiments polycrystalline materials was checked with X-ray diffraction. No phases other than the low temperature monoclinic phase of $CsHSO_4$ have been detected in starting and recovered samples.

2.2. Impedance measurements

The main difference of the present study from previous determinations of the phase transition temperatures in $CsHSO_4$ consists in the use of the impedance spectroscopy method at high pressures. The description and the calibration of the high pressure press and impedance measurements have been done elsewhere [16]. In this study a conventional end loaded piston-cylinder apparatus was used with a pressure cell consisting of CaF_2, as a confining medium, MgO insulation sleeve and the graphite sleeve as a heater [16]. The experiments have been carried out at pressures from 0.5 to 2.5 GPa and temperatures from 300 to 600 K. Additional experimental run has been conducted by using unloaded press at 0.1 MPa. The pressure calibration of the cell has been done by the use of some standard point materials: at room temperature the transformations Bi I–II–III at 2.56 and 2.7 GPa have been used; at high pressure the melting curves of NaCl and CsCl have been exploited. The melting points of these salts as a function of pressure up to 2.5 GPa has been determined *in-situ* by electrical conductivity measurements. The performed pressure calibration is believed to be within an accuracy of ± 30 MPa. For temperature measurements the S-types (at high pressures) and T-types (at low pressures) of thermocouple have been used. The temperature gradient in the cell has been estimated on $CsHSO_4$ powder samples by the use of two thermocouples located at two different distances from the center of the high pressure cell. The estimation of the radial temperature gradient is ca. 2–2.5 K/mm, the vertical temperature gradient is ca. 0.5 K/mm in the temperature range up to 600 K. The constant pressure was provided by a servomotor, which regulated the position of the piston with the help of an additional hydraulic cylinder. The oil pressure in loading hydraulic rams was maintained within ± 0.05 MPa. Movement of the compressing piston in the autoclave was monitored with the LVDT having precision ± 0.001 mm.

The electrical impedance measurements have been performed with the use of Solartron® 1260 Phase-Gain-Analyzer interfaced with PC. In the case of high resistance (>10 MΩ) the PSM 1700 Impedance Analysis Interface with the special fixture TA107 from N4L® has been used. The complex impedance data have been proceeded with the help of Novocontrol software packages WinDeta and Win Fit

The high pressure cell for the electrical impedance measurements represents a coaxial cylindrical capacitor with a geometric factor $G=4.5\text{–}6.5\times10^{-2}$ m filled with a pressed powder sample. The exact geometric factor of a cell has been evaluated as a function of frequency in calibration measurements using NaCl solutions (0.01–3 M) at 300 K and pressure 0.1 MPa [16].

During the impedance measurements the press was isolated from the ground of Phase-Gain Analyzer Solartron 1260. One of the thermocouple wires and the mass of the high pressure autoclave were used to connect the measuring device and the cell electrodes. Before doing the high pressure experiments a measuring cell has been calibrated for a short and for open circuit impedances in the frequency range from 1 MHz to 0.01 Hz. A typical AC-resistance of the cell in a short circuit is $\sim0.4\,\Omega$. These calibrations have been taken into account in final calculations of the electrical impedance as a function of frequency. Each frequency scan of the complex resistance has been fitted to the expression as follows (e.g. [17]):

$$Z^* = \frac{R_1}{1+(j\omega\tau_1)^p} + \frac{R_2}{1+(j\omega\tau_2)^n} \quad (1)$$

where the first and the second terms are responsible for high and low frequency dielectric losses, i.e. to two arcs on an Argand-type of diagram describing bulk conductivity and electrode polarization processes. In the case of the three arcs the third term has been added to Eq (1). Parameters τ_1, R_1 and p are related to the bulk properties of a sample, τ_2, R_2 and n are related to the sample-electrode polarization. The bulk DC conductivity of a sample is calculated from AC measurements $\sigma_{DC}=1/R_1G$, where G is the geometric factor of electrodes. The temperature dependence of the bulk DC conductivity usually follows an Arrhenius-type of dependence

$$\sigma_{DC}T = \sigma_0\, e^{-E_\sigma/kT} \quad (2)$$

where σ_0 is the pre-exponential factor, E_σ is the activation energy of the electrical conductivity, characterizing an energetic barrier for the movement of charge carriers, i.e. lattice defects. The parameter p in Eq (1) describes a power law dispersion in a situation when the short range displacements of lattice defects become coupled with ionic environment. In ionic conductors with the increasing temperature, p may decrease from ~1 to 0.5–0.6 [18]. In different temperature intervals the accuracy of the fitting parameters for the first or for the second terms in the right hand side of Eq. (1) varies significantly. Thus, n, τ_2 and R_2 in Eq. (2) were not used in analysis of the experimental data.

The bulk dielectric relaxation time $\tau_1=\tau$ depends on the temperature also according to an Arrhenius-type of equation as follows:

$$\tau = \tau_0\, e^{-E_\tau/kT} \quad (3)$$

where τ_0 is the pre-exponential factor and E_τ is the activation energy of the dielectric relaxation time. E_τ corresponds to the activation energy of a peak of the imaginary component of electric impedance.

2.3. Results of measurements

The results of ionic electric conductivity of measurements at 0.1 MPa, 0.5 and 0.75 GPa are presented in Fig. 1 as a graph $\ln(\sigma xT)$ vs. $1/T$. The sample measured at 0.1 MPa has been pre-compressed at 1 GPa at room temperature, and then decompressed to 0.1 MPa during ca. 72 h. Fig. 2 demonstrates the Arrhenius dependence of the dielectric relaxation time τ vs. $1/T$. The results of ^{1}H MAS NMR [19] for mean residence time τ_H are shown here for comparison as a solid arrow. The main drop of electric conductivity, of dielectric relaxation time and of mean residence time of ^{1}H corresponds to the phase transition from phase II (ferroelastic phase) to phase I (superprotonic phase). Here we use the conventional nomenclature of phases taken from [7,10,11], which is traditionally used for $CsHSO_4$ polymorphs. The range of dielectric relaxation times in phase III and II corresponds within one order of magnitude to the range of the mean residence time from ^{1}H MAS NMR [19]. At temperature above $T_c=T_{II\text{–}I}$ transition the dielectric relaxation time cannot be derived from the electrical impedance measurements. The range of dielectric relaxation times as well as the $T_{III\text{–}II}$ transition depends weakly on pressure from 0.1 MPa to 0.75 GPa (Fig. 2). The dielectric relaxation time on pressure at constant temperature increases within one order of magnitude from 0.1 MPa to 0.75 GPa. The slope of the temperature dependence of dielectric relaxation time on heating at 0.1 MPa, 0.5 and 0.75 GPa is about the same as for the temperature dependence of the mean relaxation time of protons (τ_H) estimated from NMR [19].

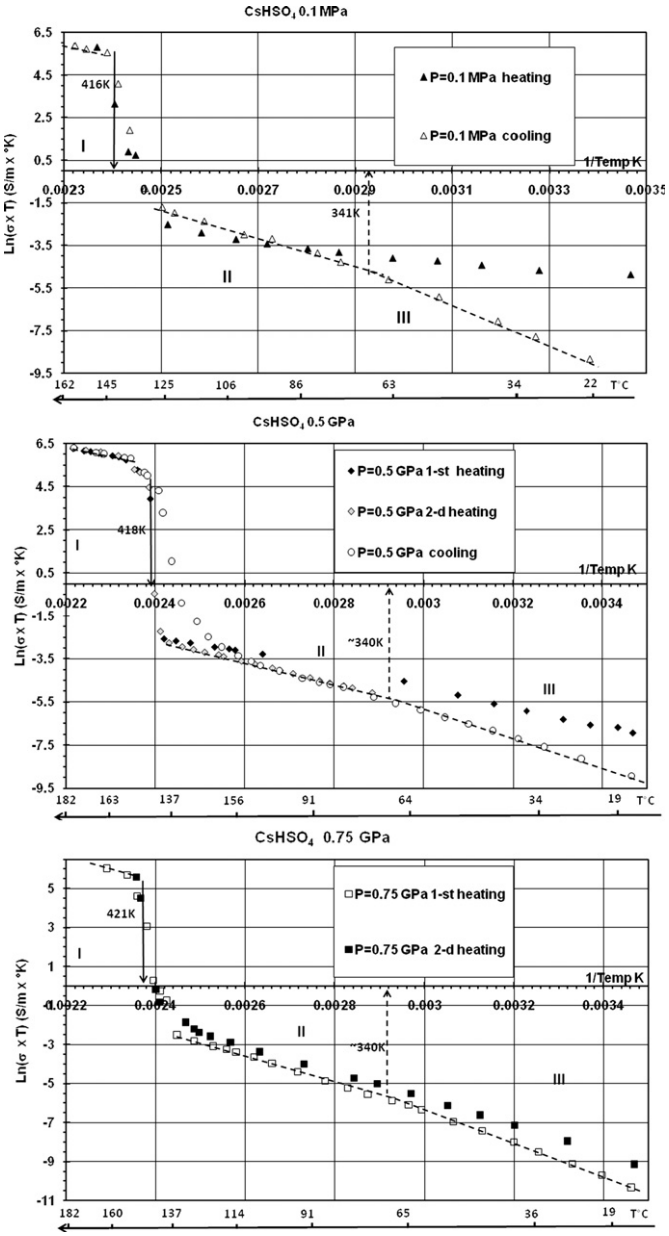

Fig. 1. Electric conductivity in $CsHSO_4$ at 0.1 MPa, 0.5 and 0.75 GPa.

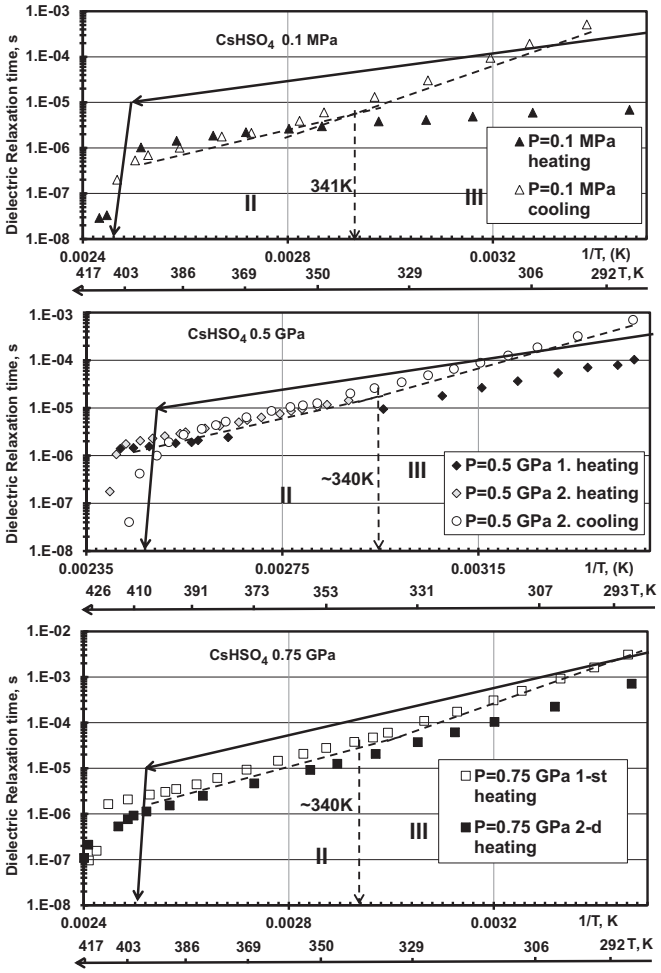

Fig. 2. Dielectric relaxation time in $CsHSO_4$ at 0.1 MPa, 0.5 and 0.75 GPa. Solid arrows indicate the drop of the mean residence time τ_H of spin–lattice relaxation [19].

The absolute values of dielectric relaxation time τ during heating are less than τ_H for about one order of magnitude at 0.1 MPa, and 0.5 orders of magnitude at 0.5 and 0.75 GPa. During cooling the dielectric relaxation time has higher activation energy than τ_H but the values of τ tend to τ_H at room temperature (Fig. 2). The absolute value of electrical conductivity measured at 0.1 MPa and 400 K is 2×10^{-4} S/m K during heating and 3.4×10^{-4} S/m K during cooling is in an agreement with the predicted ionic conductivity of phase II from proton dynamics 1.1×10^{-4} S/m K [20]. In phase III at room temperature and 0.1 MPa the measured conductivity of $CsHSO_4$ is 2×10^{-5} S/m K during heating cycle and 5×10^{-7} S/m K during cooling cycle, which is within one order magnitude of the predicted conductivity $\sim4\times10^{-6}$ S/m K at these conditions [20].

With the temperature increase from 300 K (phase III) to T_c (phase I) the impedance spectra evolve from a perfect semicircle at high frequencies with $p\approx0.90$ at room temperature to $p\approx0.80$ at 405 K (Fig. 3). This parameter characterizes the deviation of dielectric relaxation function from a Debye type of relaxation. According to Mizuno and Hayashi [20] the spin–lattice relaxation of ^{1}H is non-exponential function with the stretched exponent which varies from 0.72 at 300 K to 0.64 at 410 K. At T_c the spectrum shape change drastically. Instead of the high frequency arc shoulder in Argand-diagrams the response appears as it would be from a pure active resistance (Fig. 2). The phase transition from phase II to phase I occurs in the temperature interval of about $\Delta T\approx5$–6 K. The question is what temperature should be chosen to identify T_c? In this study T_c has been taken as a temperature at which the bulk impedance arc disappears from the impedance spectrum and the resistance of the equivalent electric circuit becomes almost active, R_1 (Fig. 3). It reversibly occurs in a temperature range within 5–6 K during heating from phase II to phase I. At these temperatures τ becomes so small that it cannot be resolved at high frequencies (Fig. 2). For example, from the evolution of the impedance spectra at $P=0.1$ MPa in Fig. 3, the phase transition from II to I is identified at $T_c=410.7\pm2.5$ K. At each pressure several consecutive heating–cooling cycles have been performed. The conductivity above T_c is fully reproducible during heating and cooling cycles (Fig. 1). The absolute value of electrical conductivity measured in phase I at 434 K and 0.1 MPa is 0.48 S/m, which is in a good agreement with previous measurements at room pressure 0.5 S/m [21] and with the theoretically predicted value from the mean residence times determined from the spin–lattice relaxation times in phase I $\sim$0.49 S/m [22].

Contrary, the electrical conductivity measured at $T<T_c$ demonstrates a significant hysteresis. The change of the slope at ca. 340 K corresponds to the irreversible phase transition in the

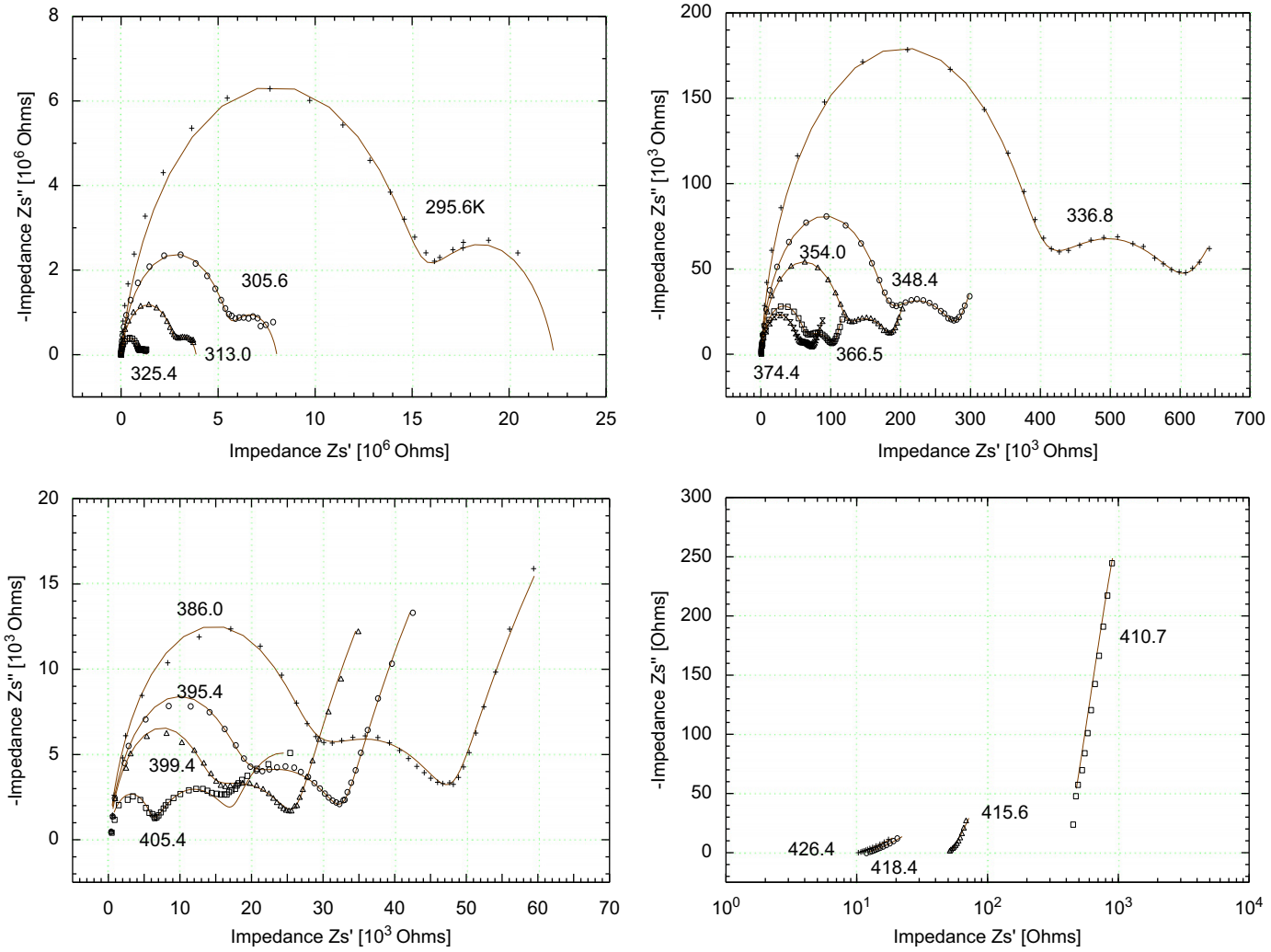

Fig. 3. Evolution of impedance spectra at $P=0.1$ MPa. The phase transition II $\Rightarrow$ I corresponds to the abrupt change of impedance spectra (right lower panel). The left arc in the Argand plots is the bulk impedance; the small intermediate arc is probably the grain boundary phase impedance. The right shoulder of the spectra is Wagner impedance branch. The parameter p from Eq. (1) varies from 0.89 at 295.6 K to 0.80 at 405.4 K.

ferroelastic phase $P2_{1/c}$ [23]. In DSC measurements [10,23] this transition has been identified as a transition from phase IV ($P2_{1/m}$) into phase III, and the transition from phase III into phase II has been assigned to the temperature interval 363–380 K. These two irreversible phase transitions have been observed only during heating, and during consecutive cooling the transitions are impeded due to the delay of spontaneous strain. After keeping the sample during several days at room temperature the low temperature transitions in ferroelastic phases appear again during heating cycles [23]. In the present experiments the transition at 340 K was also observed only during heating cycle. In earlier works with the use of constant frequency electrical conductivity measurements only one phase transition between III and II phase during heating has been observed, where temperature at room pressure varied from 323 K [7] to 333 K [24]. Essentially, the behavior of electrical impedance in $CsHSO_4$ under pressure in Fig. 1 during consecutive heating and cooling cycles is similar to what has been observed in CsH_2PO_4 [25] and in KH_2PO_4 and RbH_2PO_4 [26] at 1 GPa in the solid medium transmitting medium high pressure apparatus.

Table 1 summarizes the results of T_c determination during heating and cooling cycles in the temperature range of the phase transition from the low conductivity phase II ($P2_1/c$) into the super ionic high conductivity phase I ($I4_1/amd$). Below 0.75 GPa the electrical conductivity results presented in Fig. 1 and the determinations of T_c as a function of pressure indicated in Table 1 are similar to the previous results of DSC [27] and electrical conductivity measurements [4,11].

With the help of the present electrical impedance method the phase transition between phases III and II is identified at around 340 K in the pressure range from 0.1 MPa to 0.75 GPa, which is in disagreement with the value 330 K frequently reported in the literature [7,10,11,27–29]. The second low temperature phase transition at 375 K which was reported in [14,23,27] from DSC data, is not identified in the present study. Probably, the increase of electrical conductivity due to the increase of the excited state $H(SO_4)_2$ or $H_3(SO_4)_2$ at temperatures just below T_c hides the change of $\ln(\sigma xT)$ slope in the Arrhenius curve (Fig. 1). There is only a small kink in the slope of $\ln(\sigma xT)$ vs. $1/T$, K (Fig. 1) in the temperature range close to 370 K, but the exact position of this kink and the corresponding phase transition depends on the heating–cooling rate of a sample rather than on pressure. The DSC data measured at pressures <0.12 GPa from [14] demonstrated that the temperature of phase transition at 375 K–0.1 MPa decreases with pressure and merges with the transition at 333 K–0.1 MPa. Thus, the 340 K transition observed in this study is identified as a phase III–phase II transition. A small increase of the activation energy of electrical conductivity at the temperature

Table 1
T_c measurements of phase transition in $CsHSO_4$ from phase II to I at $P<1$ GPa and IV–VI, VI–I at $P>1$ GPa.

Pressure (GPa)	T_c on heating (K) II→I	T_c on cooling (K) I→II
0.1 MPa	410.7 ± 2.5	410.1 ± 2.5
0.5	417.6 ± 1.0	412.0 ± 2.5
0.75	419.6 ± 3.0	n.d.[a]
1.0	423.1 ± 1.2	418.9 ± 3.0
	IV→VI	VI→IV
1.5	453.6 ± 1.7	430.0 ± 1.0
2.0	511.4 ± 1.5	482.0 ± 4.5
2.5	557.0 ± 7.0	536.0 ± 3.5
	VI→I	I→VI
1.5	481.0 ± 2.5	475.0 ± 4.0
2.0	532.0 ± 4.0	521.0 ± 5.5
2.5	578.0 ± 5.0	536.0 ± 3.5

[a] Not determined.

300–400 K was observed only during the first heating of samples. The significant thermal hysteresis between heating and cooling cycles of the phase transition temperature in ferroelastic phases has been observed also in previous studies, and it was explained either as a surface phase transition [7] or as a kinetic phenomenon of spontaneous strain caused by the increase–decrease of domain size at $T<T_c$ during cooling from high temperatures [23]. A significant discrepancy of the electrical conductivity (Fig. 1) and dielectric relaxation time (Fig. 2) during the heating and cooling cycles at $T<T_c$ is obvious. The absolute values of the electrical conductivity and dielectric relaxation time vary significantly even at room temperature depending on how long the samples were kept at low temperatures. This sensitivity of electrical properties to the exposure time at room temperature can be made possible due to building of surface water-bearing phases enhancing the conduction of grain boundaries [7,27] or due to the decrease of $H(SO_4)_2$ and $H_3(SO_4)_2$ excited states with time followed by the increase of domain size and the increase of spontaneous strain in ferroelastic phases [27]. Alternatively, it may be caused by the change in a reduction degree of $CsHSO_4$ with the increasing moisture content, which activates acid centers on grain boundaries [30].

Figs. 4–7 summarize the results of electrical conductivity and dielectric relaxation time measurements obtained during two consecutive heating–cooling cycles at 1, 1.5, 2, and 2.5 GPa, respectively. At high pressures and at $T<T_c$ the kinks in slopes of $\ln(\sigma xT)$ and $\ln(\tau)$ as function of $1/T$, K which can be interpreted as phase transition boundaries, are observed only during heating cycle. This means that the pressure increase delays the effect of spontaneous strain in ferroelastic phases under cooling. During cooling the phase which appears below T_c is stable up to 300 K. Only after 1–2 days of keeping the sample at room temperature the electrical conductivity returns slowly to the values, which were measured before the last heating–cooling cycle conforming to the results of Kato et al. [23] obtained at 0.1 MPa.

3. Discussion

The calculated slopes or the activation energies of the bulk electrical conductivity σxT (E_σ) and dielectric relaxation time τ (E_τ) at $P<1$ GPa are summarized in Table 2 and at $P>1$ GPa in Table 3. The activation energy of E_σ or E_τ may be used as an indirect marker of phases to be identified from the electrical impedance measurements.

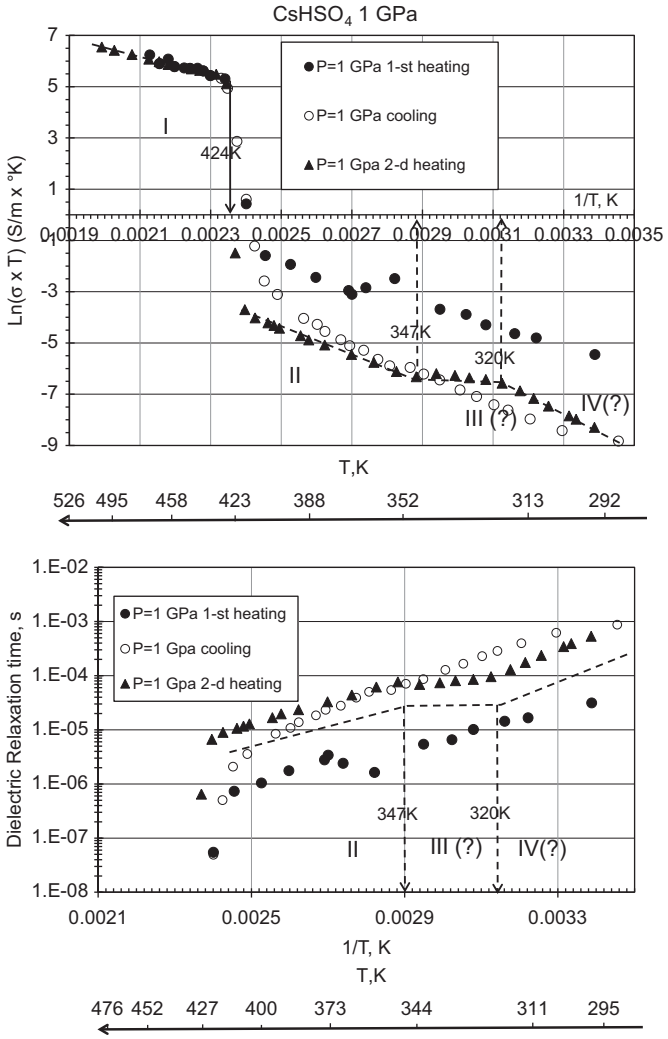

Fig. 4. Electrical conductivity σ and dielectric relaxation time τ at 1 GPa: phase I is superprotonic, phases II–IV are ferroelastic.

In the present study the slope of phase boundaries IV–VI and VI–I is about 100–105 K/GPa in comparison with 63–65 K/GPa reported in [4]. From the electrical conductivity data, it is not possible to identify the location of phase boundary of the intermediate super ionic phase VII during the heating cycle (Figs. 6 and 7). The heating and cooling paths are very different at $P>1$ GPa in contrast to the measurements at $P<1$ GPa. At high temperatures $T>T_c$ the activation energy is $E_\sigma\sim0.37\pm0.05$ eV at $P<1$ GPa and $E_\sigma\approx0.30\pm0.05$ eV at $P>1$ GPa. This value of E_σ at $T>T_c$ is practically independent on pressure. For phase II the activation energy is ca. 0.52 eV and for phase III 0.70 eV (Table 2). From other side, the ^{1}H MAS NMR data [11] demonstrated about the same activation energy for the proton mean residence time $\sim$0.36 eV in superprotonic phase at room pressure and twice less activation energy 0.26 eV in ferroelastic phase $CsHSO_4$ (II). In [19] these results have been reproduced, the values 0.35 and 0.3 eV for superprotonic and phase II were reported, respectively. This means that in superprotonic phase I the density of mobile protons is fixed and does not depend on pressure and temperature, $N=8.48\times10^{27}$ m^{-3} which was calculated from the crystal structure [19]. Thus, the super ionic phase I is a typical protonic conductor, which appears above T_c. The measured values of the

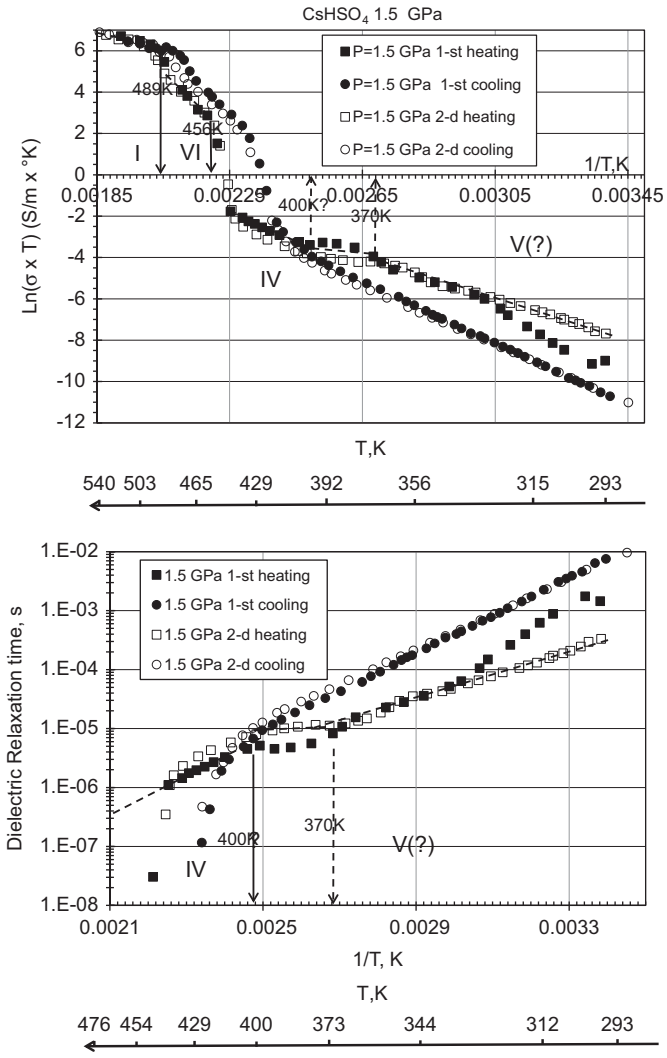

Fig. 5. Electrical conductivity σ and dielectric relaxation time τ at 1.5 GPa: phases I and VI are superprotonic, phases V and IV are ferroelastic.

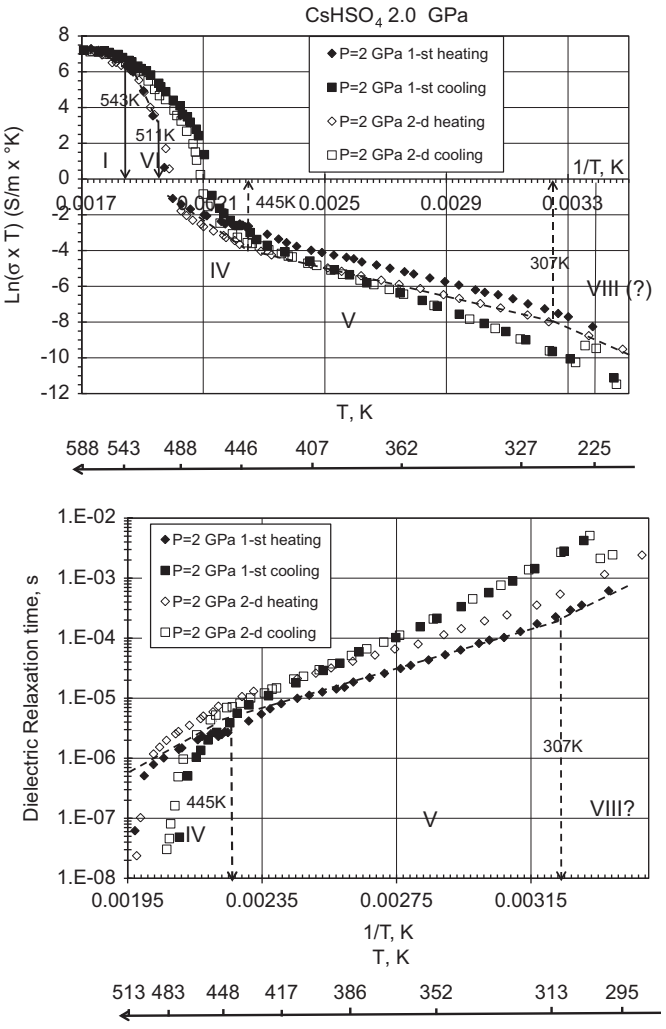

Fig. 6. Electrical conductivity σ and dielectric relaxation time τ at 2 GPa: phases I and VI are superprotonic, phase V is ferroelastic, Phase VIII is not ferroelastic.

activation energy E_σ are slightly higher than the previously reported values of the activation energy of electrical conductivity 0.31 eV [11], 0.28 eV [21] and 0.27 eV [31]. The phase II ($P2_1/c$) which exists below 330 K and at pressures below 1 GPa, $E_\sigma \sim 0.75$–0.60 eV, which is in agreement with the reported values $E_\sigma \sim 0.76$–0.79 eV according to Shin [31]. This value is twice higher than the activation energy of the mean residence time of protons or the mobility activation energy ~ 0.3 eV, which means that the number of mobile protons varies with temperature below T_c, and the activation energy of this process is about 0.3–0.45 eV. In phase IV ($P2_1/m$) the activation energy is about $E_\sigma \sim 0.6$–0.5 eV, close to the values of the phase II.

The identification of the phase boundaries between low conductivity phases with the use of electrical conductivity measurements is not so straightforward. Due to the small differences in slopes of $\ln(\sigma xT)$ and $\ln(\tau)$ as a function of $1/T$, K, these phases have a negligible difference of activation energies (Table 2). The phase IV or the second phase transition in ferroelastic phases as it is sometimes mentioned in the literature [23], was not observed under pressure <1 GPa which is in agreement with the results of Baranowski et al. [14]. The significant decrease of the phase transition temperature from phase III into phase II at low pressures (<0.1 GPa) mentioned in [14] is not supported by the present measurements (Fig. 1).

The electrical conductivity mechanism in phases I, II, and III has been discussed in [6,11,32,33]. The high conductivity and the relatively low activation energy of the fast ionic conductor phase I is provided by two simultaneously acting processes, the reorientation of HSO_4 groups having the activation energy ca. 0.35 eV, and the long range translation diffusion of protons along hydrogen bonds having the activation energy 0.25 eV [11,23,33]. In phase III the hydrogen bonds are stronger than in phase II, the lattice is rigid. With the temperature increase the spin–lattice relaxation time decreases and the spin–spin relaxation time increases. During the inversion from phase III into phase II the transition temperature corresponds to an abrupt decrease and an increase of longitudinal and transversal decay constants of NMR [32]. The relaxation of the rotating frame decay constant has a minimum at 375 K. Thus, 375 K phase transition may be considered as a kinetic pseudo-glass transition, which is effectively suppressed under pressure. In superprotonic phase I reorientational and translational decay constant are equal, the temperature increase results in averaging of the anisotropic interactions of HSO_4^- ions. The activation energy of electrical conductivity along the crystallographic axes b and c in phase II ($P2_1/c$) phase are 0.73 and 0.97 eV in comparison with 0.25 and 0.28 eV in the phase I ($I4_1/amd$) [34]. Thus, with the temperature increase the number of mobile protons increases gradually at $T > 330$ K and reaches a constant value in phase II [6]. In phase I at $T > T_c$ the number of mobile protons which could hop from one hydrogen bond to another remains constant but their mobility

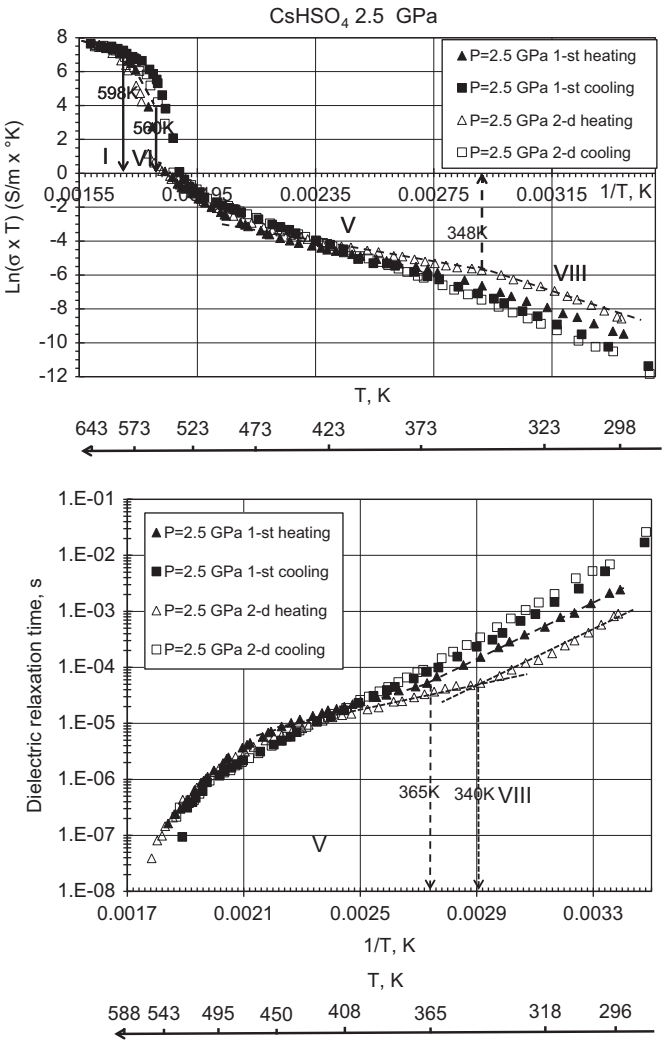

Fig. 7. Electrical conductivity σ and dielectric relaxation time τ at 2.5 GPa, phases V and VIII are probably not ferroelastic, small knick in slope is observed during cooling cycle.

Table 2
Activation energies from IS measurements at $P<1$ GPa.

Pressure (GPa)	$T<T^1$	$T^1<T<T_c$	$T>T_c$
0.1 MPa			
($T^1=T_{II-III}\sim340$ K)	0.75[a]/0.7[b]	0.57[a]/0.52[b]	0.37[a]
0.5			
($T^1=T_{II-III}\sim340$ K)	0.73/0.72	0.58/0.54	0.36
0.75			
($T^1=T_{II-III}\sim340$ K)	0.62/0.60	0.58/0.60	0.37
1.0			
($T^1=T_{II-IV}\sim370$ K)	0.40/0.38	0.50/0.45	0.33

[a] E_σ of $\sigma_{DC}\times T$ bulk conductivity in eV calculated from Eq. (2).
[b] E_τ of τ in eV dielectric relaxation time from Eq (3).

increases drastically due to the activated reorientation movement of SO_4^{2-} tetrahedra. From the present high pressure measurements of electrical conductivity it seems that the pressure does not have any effect on this process. The increased disordering of SO_4^{2-} tertrahedra with the temperature increase plays a crucial role in the enhanced conductivity of phase I, the thermal disordering of protons itself is of minor importance [33].

Nevertheless, if one judges from the results of activation energy of electrical conductivity and dielectric relaxation time at 1 GPa the phase, which exists at $T<370$ K is different from phase III occurring at lower pressures. According to the classification of [7,28,29,34,35] this is probably phase IV ($P2_1/m$), possessing the activation energy E_σ ca. 0.4 eV. The same phase is observed at 1.5 GPa at 375 K $<T<$ 454 K and at 2.0 GPa at 445 K $<T<$ 515 K. Phase III at $P=1$ GPa was not observed at low temperatures $T<330$ K. In [23,35] the irreversible transformation of phase II into III (or IV) at 0.75–1.1 GPa has been explained due to the pressure stabilization effect of the phase II structure. At 1.25 GPa phase II transforms into phase IV [36]. Under cooling the domain size of phase II, which is transformed from phase I, is small, and this causes a kinetic delay of the phase II into low temperature phase. During annealing over 2–3 days at low temperatures $T\sim300$ K and at high pressures $P=0.5$–1 GPa, the ferroelastic phases III and IV have been observed again judging from the activation energy of the electrical conductivity E_σ during second heating cycle (Figs. 1 and 4).

Phase V observed at room temperature at $P>1.4$ GPa is monoclinic $P2_1/m$ or $P2_1$ [36], and in the present experiments appeared at 1.5 GPa having the activation energy of electrical conductivity $E_\sigma\sim0.63$ eV. Phase VI is the intermediate superprotonic phase with *Pnma* symmetry [36] has been observed in this study at $P>1.5$ GPa possessing the activation energy of electrical conductivity $E_\sigma\sim1.4$ eV (Table 3).

At 2.5 GPa the phase which exists at room temperature is different from that at 2.0 GPa. This probably corresponds to phase VIII, whose existence has been suggested in [29]. The phase transforms into phase V at 350 K. At pressures 1.5–2.5 GPa the jump of electrical conductivity from the low conductive ferroelastic phases into the fast protonic conductor phase occurs in two steps (Figs. 5–7), which has been observed also in previous studies [4,7]. At 2.5 GPa during cooling between phases I and VI there is a temperature interval 570 K $<T<$ 585 K where the activation energy is $E_\sigma\sim0.8$–1.0 eV (Fig. 7). This can be interpreted as an occurrence of the intermediate fast ionic conductor phase VII, but even upon heating the jump of electrical conductivity is negligible, so this phase was practically undistinguishable.

The phase transition boundaries between low conductivity phase II and super ionic phase I at $P<1$ GPa identified from electrical conductivity measurements are indicated in Table 1 and summarized in Fig. 8 (upper panel). The Clapeyron slope of the phase boundary between phases II and I at low pressures $dT_c/dP\sim10$ K/GPa which is in a good agreement with previous studies [4,9,25]. Thus, the phase boundaries of $CsHSO_4$ at $P<1$ GPa are not very much different from previous results (Fig. 8, upper panel). The main difference of the results of this study from previous measurements [4] is in the location of phase transition boundaries at $P>1$ GPa (Fig. 8 upper panel). According to [4], in which the electrical measurements were carried out at a fixed 1 kHz frequency, the phase transition II–I splits with the appearance of the second intermediate high conductive phase VI. The slopes of the both transitions IV–VI and VI–I were determined in [4] as about 65 K/GPa. In this study this phase boundary slope is ~100 K/GPa. At pressure about 1.8 GPa another intermediate superionic phase VII was reported in [4], which appears between the phase boundaries of phases VI and I. There is no firm confirmation of the existence of phase VII from this study, and this phase may occur at higher temperatures and pressures.

The phase boundaries between the low conductive phases are poorly determined in this study. In the lower panel of Fig. 8 the temperatures, which correspond to the probable phase transitions are plotted as a tentative phase diagram. The interpretations of kinks in slopes of $\ln(\sigma xT)$ vs. $1/T$ were made on the basis of the previous experimental phase diagram [4]. The indicated phase boundaries are more conforming to recent experimental results of [10,36,37] rather than to results of [4]. Phase IV is stable at

Table 3
Activation energies from IS measurements at $P>1$ GPa.

Pressure (GPa)	$T<T_1$	$T^1<T<T^2$	$T^2<T<T_c$	$T>T_c$
1.5 ($T^1=T_{V-IV}\sim375$ K, $T^2=T_{IV-VI}\sim454$ K)	0.63/0.65	0.31/0.33	1.40	0.32
2.0 ($T^1=T_{V-IV}\sim445$ K, $T^2=T_{IV-VI}\sim515$ K)	0.55/0.56	0.40/0.38	1.35	0.30
2.5 ($T^1=T_{VIII-V}\sim350$ K, $T^{2*}=T_{V-IV}\sim460$ K, $T^3=T_{V-IV}\sim505$ K)	0.50/0.49	0.31/0.29 $T^{2*}<T<T^3$ 0.65/0.60	1.70	0.31

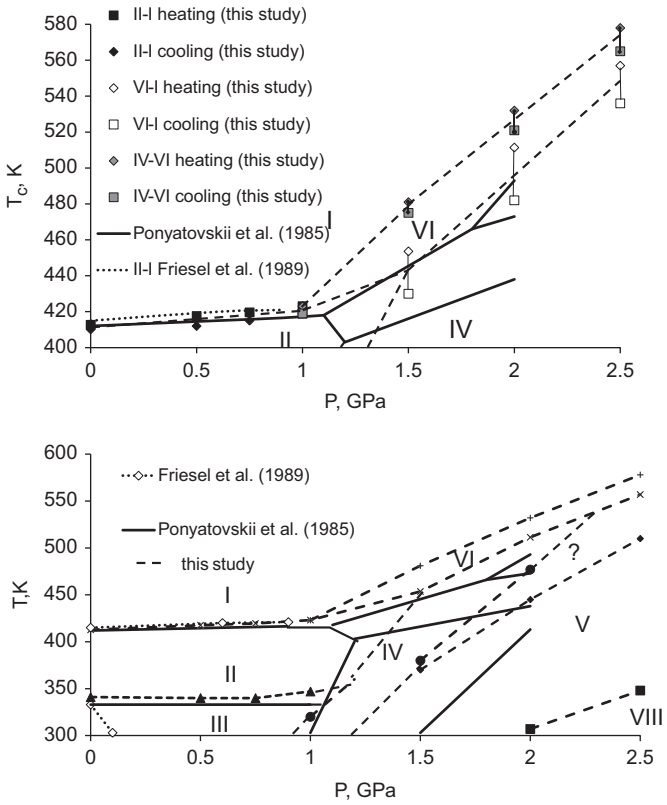

Fig. 8. Phase diagram derived from electrical impedance measurements in comparison with the previous data [4,9]: upper panel represents phase transitions in superprotonic phases; lower panel represents a tentative diagram of phase transitions in ferroelastic phases based on electrical impedance measurements of this study.

1.25 GPa and room temperature [36], phase II is stable in the range 0.75–1.1 GPa [37]. It should be noted here that *in situ* determinations of phases are highly needed for the interpretation of electrical conductivity measurements at high pressure.

4. Conclusions

The IS measurements on polycrystalline $CsHSO_4$ at pressure up to 2.5 GPa have confirmed the location of the phase boundary II–I at $P<1$ GPa. This study also demonstrated that the high pressure phase boundaries at $P>1$ GPa are different from the previous results [4]:

1. The reversible phase transition from phase II into phase I is observed at pressures from 0.1 MPa to 0.75 GPa with the Clapeyron slope $dT_c/dP\sim10$ K/GPa. The activation energy of the electric conductivity and dielectric relaxation time in phase I is ca. 0.35 eV and, which is equal to the mean residence time of protons. This value seems to be independent on pressure.
2. The Clapeyron slope of the reversible phase transition from the super ionic phase VI into phase I at $P>1$ GPa is ~100 K/GPa.
3. The intermediate fast ionic conductor phase VI possesses the activation energy $E_s\sim1.4$ eV and the Clapeyron slope of the transformation of phase VI into phase IV is also ~100 K/GPa.
4. The phase VII which has the activation energy $E_s\sim0.8$–1.0 eV appears only during cooling from phase I.
5. At 2.5 GPa below 350 K phase VIII is observed with the activation energy of electrical conductivity ca. 0.5 eV.

Acknowledgement

The author is thankful to M. Lutschitzkaya for the synthesis of $CsHSO_4$ samples.

References

[1] K.-D. Kreuer, Chem. Mater. 8 (1996) 610.
[2] S.M. Haile, Acta Mater. 51 (2003) 5981.
[3] M. Komukae, T. Osaka, Y. Makita, T. Ozaki, K. Itoh, E. Nakamura, J. Phys. Soc. Jpn. 50 (1981) 3187.
[4] E.G. Ponyatovskiĭ, V.I. Rashchupkin, V.V. Sinitsyn, A.I. Baranov, L.A. Shuvalov, N.M. Shchagina, JETP Lett. 41 (1985) 139.
[5] M. Pham-Thi, Ph. Colomban, A. Novak, R. Blinc, Solid State Commun. 55 (1985) 265.
[6] Y. Yoshida, Y. Matsuo, S. Ikehata, J. Phys. Soc. Jpn. 72 (2003) 1590.
[7] A.I. Baranov, V.V. Sinitsyn, E.G. Ponyatovskiĭ, L.A. Shuvalov, JETP Lett. 44 (1986) 237.
[8] E. Ortiz, R.A. Vargas, B.-E. Mellander, J. Phys.: Condens. Matter 18 (2006) 9561.
[9] B. Baranowski, J. Lipkowski, A. Lundén, J. Solid State Chem. 117 (1995) 412.
[10] A. Lundén, B. Baranowski, M. Friesel, Ferroelectrics 167 (1995) 33.
[11] V.V. Sinitsyn, A.I. Privalov, O. Lips, A.I. Baranov, D. Kruk, F. Fujara, Ionics 14 (2008) 223.
[12] D.A. Boysen, C.R.I. Chisholm, S.M. Haile, S.R. Narayanan, J. Electrochem. Soc. 147 (2000) 3610.
[13] V.G. Ponomareva, G.V. Lavrova, Solid State Ionics 145 (2001) 197.
[14] B. Baranowski, M. Friesel, A. Lundén, Physica A 156 (1989) 353.
[15] C. Chisholm, S.M. Haile, Chem. Mater. 19 (2007) 270.
[16] N. Bagdassarov, C.-H. Freiheit, A. Putnis, Solid State Ionics 143 (2001) 285.
[17] A.K. Jonscher, J. Phys. D: Appl. Phys. 32 (1999) R57.
[18] D.L. Sidebottom, P.F. Green, R.K. Brow, Phys. Rev. Lett. 74 (1995) 5068.
[19] Y. Daiko, S. Hayashi, A. Matsuda, Chem. Mater. 22 (2010) 3418.
[20] M. Mizuno, S. Hayashi, Solid State Ionics 167 (2004) 317.
[21] T. Norby, M. Friesel, B.E. Mellander, Solid State Ionics 77 (1995) 105.
[22] S. Hayashi, M. Mizuno, Solid State Ionics 171 (2004) 289.
[23] T. Kato, J. Hatori, Y. Yoshida, Y. Matsuo, S. Ikehata, Solid State Ionics 178 (2007) 735.
[24] A.I. Baranov, L.A. Shuvalov, N.M. Shchagina, JETP Lett. 36 (11) (1982) 381.
[25] D.A. Boysen, S. Haile, H. Liu, R.A. Secco, Chem. Mater. 15 (2003) 727.
[26] D.A. Boysen, S. Haile, H. Liu, R.A. Secco, Chem. Mater. 16 (2004) 693.
[27] M. Friesel, B. Baranowski, A. Lundén, Solid State Ionics 35 (1989) 85.
[28] N.M. Plakida, V.S. Shakhmatov, Ferroelectrics 167 (1995) 73.
[29] V.S. Shakhmatov, High Pressure Res. 14 (1995) 67.
[30] V.G. Ponomareva, G.V. Lavrova, Inorg. Mater. 45 (2009) 85.
[31] H.K. Shin, Solid State Ionics 179 (2008) 2101.

[32] A. Damyanovich, M.M. Pintar, R. Blinc, J. Slak, Phys. Rev. B 56 (1997) 7942.
[33] S. Hayashi, M. Mizuno, Solid State Commun. 132 (2004) 443.
[34] A.I. Baranov, B.V. Merinov, A.V. Tregubchenko, V.P. Khiznichenko, L.A. Shuvalov, N.M. Schagina, Solid State Ionics 36 (1989) 279.
[35] A.V. Belushkin, M.A. Adams, S. Hull, A.I. Kolesnikov, L.A. Shuvalov, Physica B 213&214 (1995) 1034.
[36] A.V. Belushkin, M.A. Adams, S. Hull, L.A. Shuvalov, Solid State Ionics 77 (1995) 91.
[37] A.V. Belushkin, T. Mhiri, S.F. Parker, Physica B 234-236 (1997) 92.